

Information-Based Path Planning for UAV Coverage with Discrete Measurements

Nicolas Bono Rossello^{1,2} Renzo Fabrizio Carpio² Andrea Gasparri² Emanuele Garone¹

Abstract—This paper presents a novel information-based mission planner for a drone tasked to monitor a spatially distributed dynamical phenomenon. For the sake of simplicity, the area to be monitored is discretized. The insight behind the proposed approach is that, thanks to the spatio-temporal dependencies of the observed phenomenon, one does not need to collect data on the entire area. In fact, unmeasured states can be estimated using an estimator, such as a Kalman filter. In this context the planning problem becomes the one of generating a flight path that maximizes the quality of the state estimation while satisfying the flight constraints (e.g. flight time). The first result of this paper is to formulate this problem as a special Orienteering Problem where the cost function is a measure of the quality of the estimation. This approach provides a Mixed-Integer Semi-Definite formulation to the problem which can be optimally solved for small instances. For larger instances, two heuristics are proposed which provide good sub-optimal results. To conclude, numerical simulations are shown to prove the capabilities and efficiency of the proposed path planning strategy. We believe this approach has the potential to increase dramatically the area that a drone can monitor, thus increasing the number of applications where monitoring with drones can become economically convenient.

Index Terms—Unmanned Aerial Vehicles, Path Planning, Kalman Filter, Optimization.

I. INTRODUCTION

UNMANNED aerial vehicles (UAVs) are commonly used to perform field coverage activities. These vehicles are typically equipped with a large variety of sensors to take measurements of areas of interest. Applications for these kind of systems include monitor operations in agriculture [1], archaeology [2] and civil infrastructures [3].

In many applications, remote sensing best practices use post-processed information in the form of an orthomosaic [4]. An orthomosaic is essentially a geometrically corrected image obtained thanks to the composition of several overlapped photographs [5]. This technique implies an exhaustive and complete coverage of the area, commonly using boustrophedon patterns as the one shown in Fig. 1. However, in the case of precision farming or other monitoring domains, the creation of a complete orthomosaic can be extremely time consuming, and might require several flights to cover relatively

This work has been supported by the European Commission under the Grant Agreement number 774571(project PANTHEON- "Precision farming of hazelnut orchards")

¹Service d'Automatique et d'Analyse des Systèmes: Université Libre de Bruxelles (ULB), Av. F.D. Roosevelt 50, CP 165/55, 1050 - Brussels, Belgium. Email: {nbonoros, emgarone}@ulb.ac.be

²Department of Engineering: Roma Tre University, Via della Vasca Navale, 79/81 00146 - Rome, Italy. Email: renzo.carpio@uniroma3.it, gasparri@dia.uniroma3.it

small areas, thus limiting the real world applicability of drones. To understand the dimension of the problem, it is worth to mention the experience of the H2020 EU project PANTHEON "Precision farming of hazelnut orchards" where the farming area is several hundreds of hectares while the area that can be covered using a boustrophedon approach is less than half a hectare for each flight.

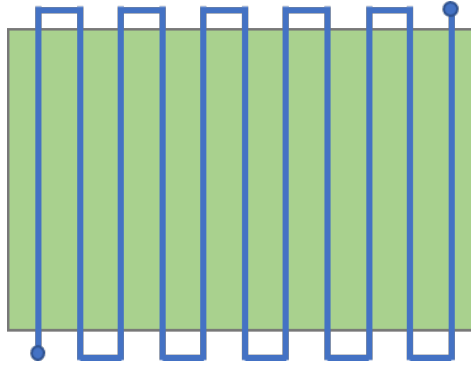


Fig. 1: Example of a boustrophedon pattern used for remote sensing.

Given this common limitation in time and resources, the literature has focused on the definition of optimal policies that partially cover the area of interest. In this regard, many persistent monitoring works rely on graph-based strategies where the latency in between visits to every region is minimized [6], [7], [8]. However, these strategies consider a static and node-independent distribution of the phenomena, which makes them non suitable for physical systems with significant dynamics.

Alternative approaches base their policies on the spatial correlation between the measurements. In these works, the mission path is computed such it avoids redundant data and thus gathers the maximum amount of information per flight. In [9], UAVs equipped with omnidirectional sensors perform an information-based exploration where the goal is to minimize the time to obtain a predefined measure of data. In environment monitoring, the monitored strategy is defined such that the measurement uncertainty of a Gaussian Process (GP) regression is minimized [10]. Also in the field of autonomous underwater vehicles (AUVs), multiple AUVs are used to perform the sampling of a scalar field based on the information obtained [11]. These works optimize the path regarding the spatial distribution of the possible measurements. Yet they tend to fail in the evaluation of the temporal correlation with previous data information, which is a meaningful aspect in most persistent monitoring activities.

In the presented paper, we assume that the phenomena to be monitored have dynamics and statistical properties which are known, e.g. water distribution [12], [13] or dust deposition [14], [15]. Thus, a good monitoring policy must address these aspects in the definition of the UAV path planning. In our work, we propose a path planning strategy where the area of interest is only partially covered and the remaining elements are estimated based on the dynamics of the system and the spatial correlation between measurements. This approach resembles to a sensor selection problem [16], [17] where the measurement points are considered as the selection or not of available sensors in the observer formulation.

In this regard, the literature presents a few examples of path planning for spatio-temporal phenomena monitoring [18], [19], [20]. Binney *et al.* [18] defines a recursive greedy algorithm to compute waypoints based on a given indicator of the estimation process. As example, given a Gaussian Process, the covariance of the estimation of different areas is minimized during a sensing exploration using AUVs. In Garg *et al.* [19], the authors assume a stochastic dynamic system and perform a multi-vehicle sampling where each robot moves such that the entropy of a particles filter is maximized. Lan *et al.* [20] models the phenomena as Gaussian processes and defines periodic trajectories to minimize the largest eigenvalue of the covariance of a Kalman Filter.

In this paper, the path planning policy is obtained as part of the estimation process of the monitored phenomena. This is achieved by structuring it as an Orienteering Problem (OP) [21]. The Orienteering Problem is a combinatorial problem which consists of a node selection where the shortest path in between the selected nodes is determined. Given a time or length constraint, the objective is to maximize the score given by the visited points. UAV remote sensing activities, due to the flight time restriction and the discrete nature of the measurements, are likely to be adapted as an OP. In this context, the set of points represents the possible measurement coordinates, the time interval is adapted to the vehicle autonomy, and the cost function is some measure related to the measurement point.

Related works in path planning already rely on an Orienteering problem framework to define tentative information-based policies for monitoring activities. In [22], the information obtained is maximized using a quadratic utility function to represent the spatial relation between the different measurement points. More recently, Bottarelli *et al.* [23] introduces an Orienteering-based path planning used to optimize a level set estimation. In this work, the measurement points are selected such the accuracy of the level sets classification is maximized.

The main contribution of this paper is the inclusion of the update step of the Kalman filter estimation as part of the Orienteering Problem. This is done by resorting to a formulation based on the Fisher information matrix. The main advantage of this approach is that the path of the mobile sensor is computed taking into account the process dynamics, the estimation uncertainty and the existing fixed sensing structure. By doing so, it allows to define the optimal combination of the UAV remote sensing with additional sensing devices by resorting to an observer-based architecture.

The developed strategy provides an offline computation of

the optimal sensing areas over one step ahead horizon of the estimation process. This approach allows to obtain the optimal path in cases where the coverage is done with unknown periodicity or when the time gap between flights is too large.

In order to solve the stated problem we propose a Mixed-Integer Semi-Definite Programming (MISDP) formulation where the minimum eigenvalue of the information matrix is maximized. This formulation allows to obtain the optimal solution for small instances of the problem. Additionally, for the case of large-scale scenarios, two heuristics are proposed along with an exhaustive computational analysis.

The remainder of the paper is organized as follows. In Section II, the problem is stated and defined. Section III provides the proposed estimation measure to monitor the phenomena and Section IV introduces the problem formulation for the information-based path planning. In Section V, the two heuristics strategies are introduced. Section VI presents a study of the performance of both heuristics and in Section VII more simulations tests are performed comparing their performance with traditional strategies. To end up the paper, in Section VIII, conclusions and future works are given.

II. PROBLEM SETTING

Consider a plane partitioned in N areas and let the linear time invariant system

$$x_{k+1} = Ax_k + Bu_k + w_k \quad (1)$$

describe the dynamic phenomenon that we want to observe. We assume that the state vector is in the form

$$x_k = \begin{bmatrix} x_k^1 \\ \vdots \\ x_k^N \end{bmatrix}$$

where $x_k^i \in \mathbb{R}^n$ represents the states of the system in the i th area and $u_k \in \mathbb{R}^n$ is the vector of the (measured) inputs to the system. A, B are matrices of consistent dimensions. The system is subject to a process disturbance $w_k \sim N(0, Q)$ modelled as a stochastic Gaussian noise with covariance $Q \in \mathbb{R}^{nN \times nN}$, which is typically non-diagonal and has nonzero terms for variables describing adjacent areas.

To estimate the state of this process, two classes of sensors are assumed available: fixed sensors and mobile sensors. We denote with $C_i \in \mathbb{R}^{M_i \times n}$ the measurement matrix associated to the measurements that can be potentially performed on the i th area. This matrix consists of two sub-matrices

$$C_i = \begin{bmatrix} C_i^f \\ C_i^m \end{bmatrix} \quad \forall i = 1, \dots, N, \quad (2)$$

where $C_i^f \in \mathbb{R}^{f_i \times n}$ denotes the available fixed measurements of the i th area and $C_i^m \in \mathbb{R}^{m_i \times n}$ is the matrix associated to the outputs that can be measured if the area is visited by a mobile sensor.

The combination of the measurement matrices of each area provides a time-invariant observation matrix $C \in \mathbb{R}^{M \times Nn}$ in the form of a block-diagonal matrix,

$$C = \begin{bmatrix} C_1 & \dots & O_{M_1 \times n} \\ \vdots & \ddots & \vdots \\ O_{M_N \times n} & \dots & C_N \end{bmatrix}, \quad (3)$$

which defines the information of the system that can be accessed to through the two classes of sensors.

To represent the fact that at a time k an area might or might not be visited by the mobile sensor, we introduce the binary variable γ_k^i . In particular, $\gamma_k^i = 1$ if the i th area is visited at time k , and $\gamma_k^i = 0$ otherwise. Accordingly, we define the measurement selection matrix Γ_k^i corresponding to each area as

$$\Gamma_k^i = \begin{bmatrix} I_{f_i \times f_i} & O_{f_i \times m_i} \\ O_{m_{i,k} \times f_i} & I_{m_{i,k} \times m_{i,k}} \end{bmatrix}, \quad (4)$$

where $m_{i,k} = \gamma_k^i m_i$. In other words

$$\Gamma_k^i = \begin{cases} \begin{bmatrix} I_{f_i \times f_i} & O_{f_i \times m_i} \\ O_{m_{i,k} \times f_i} & I_{m_{i,k} \times m_{i,k}} \end{bmatrix} & \text{if } \gamma_k^i = 1 \\ \begin{bmatrix} I_{f_i \times f_i} & O_{f_i \times m_i} \\ O_{m_{i,k} \times f_i} & I_{m_{i,k} \times m_{i,k}} \end{bmatrix} & \text{if } \gamma_k^i = 0. \end{cases} \quad (5)$$

Given this, the selection of the available measurements at time k is provided by the matrix $\Gamma_k \in \mathbb{R}^{M_k \times M}$, which is computed as

$$\Gamma_k = \Gamma_k^1 \oplus \Gamma_k^2 \oplus \dots \oplus \Gamma_k^N = \begin{bmatrix} \Gamma_k^1 & \dots & O_{M_1 \times n} \\ \vdots & \ddots & \vdots \\ O_{M_N \times n} & \dots & \Gamma_k^N \end{bmatrix}, \quad (6)$$

where \oplus denotes the direct sum operator and M_k represents the number of measurements available at time k .

Using this matrix we can write the measurement equation of the entire system as

$$y_k = \Gamma_k(Cx_k + v_k), \quad (7)$$

where $y_k \in \mathbb{R}^{M_k}$ is the set of measurements available to the system at time k and where v_k represent the measurement noise, which is assumed to be a stochastic Gaussian noise $v_k \sim N(0, R)$ with diagonal covariance matrix $R \in \mathbb{R}^{M \times M}$.

Due to autonomy limitations, at each sampling time the mobile sensor can collect information only on a limited amount of areas. To model this, in this paper we will consider the following reasonable approximations concerning the mobile sensor:

- The visit of an area is equivalent to the visit of its centroid;
- At each time k the mobile sensor has a limited maximum autonomy $T_{max,k} > 0$ (e.g. in the case of a UAV this is the flight time);
- The budget of autonomy that is spent to go from the centroid of the area i to the centroid of the area j is a fixed quantity t_{ij} (in the case of a UAV the time to travel from i to j).

Accordingly, we can define the mobile sensor's trajectories as a path on an undirected and connected graph $G = \langle V, E \rangle$ where the $V = \{0, 1, 2, \dots, N, N+1\}$ and $E \subset V \times V$, are the set of vertices and arcs, respectively.

The vertices $1, \dots, N$ represent the labels of the centroids of each area, while the vertices 0 and $N+1$ represent pre-defined starting and ending positions for each mission (in the case of a UAV are the takeoff and the landing pads).

Concerning the edges, in line of principle any set of arcs that makes the graph E connected can be selected. In this paper, without any loss of generality, we will focus on the

realistic case that $(0, j) \in E, (j, N+1) \in E, \forall j = 1, \dots, N$ and that an edge (i, j) with $i, j \in \{1, \dots, N\}$ exists only if the i th area and the j th area are adjacent. Each edge $(i, j) \in E$ have an associated weight t_{ij} representing the amount of autonomy spent to travel from vertex i to vertex j . The overall graph is depicted in Figure Fig. 2.

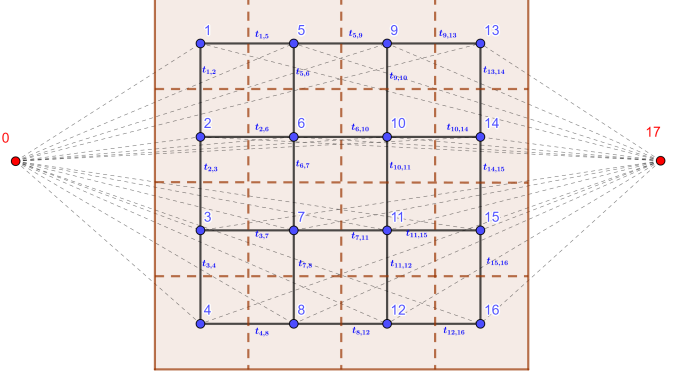


Fig. 2: Example of the regular grid obtained for a monitored area.

The goal of this paper is to compute at each sampling time k a feasible path for the mobile sensor such that some measure of the information collected is maximized given the limited autonomy of the vehicle. In other words, we want to determine an ordered sequence of nodes

$$S_k = [s_1, s_2, \dots, s_{n_k}] \quad (8)$$

where

$$s_1 = 0, \quad (9)$$

$$s_{n_k} = N+1, \quad (10)$$

$$(s_i, s_{i+1}) \in E \quad i = 0, \dots, n_k - 1, \quad (11)$$

such that

$$\sum_{i=1}^{n_k-1} t_{s_i, s_{i+1}} \leq T_{max,k}, \quad (12)$$

which maximizes some measure of the collected information. In the next section we will characterize the measure of the information to be maximized.

III. ESTIMATION OF THE MONITORED SYSTEM

Since system (1) is a linear system subject to Gaussian noise, and given the occasional availability of the mobile sensing, the most natural choice to estimate the state is the Kalman filter with intermittent observations (see [24], [25]) which is the optimal estimator for this kind of systems.

The prediction step of this estimator is

$$\hat{x}_{k|k-1} = A\hat{x}_{k-1|k-1} + Bu_k \quad (13)$$

$$P_{k|k-1} = AP_{k-1|k-1}A^T + Q, \quad (14)$$

and the correction step is

$$\hat{x}_{k|k} = \hat{x}_{k|k-1} + K_k(y_k - C_k\hat{x}_{k|k-1}) \quad (15)$$

$$K_k = P_{k|k} C_k^T (C_k P_{k|k-1} C_k^T + R_k)^{-1} \quad (16)$$

$$P_{k|k} = P_{k|k-1} - K_k C_k P_{k|k-1}, \quad (17)$$

where $\hat{x}_{k|k}$ is the estimated value of the state at time k given the information available at that time and $P_{k|k}$ is the error covariance matrix of the estimation. The time-variant matrices C_k and R_k are defined as $C_k = \Gamma_k C$ and $R_k = \Gamma_k R \Gamma_k^T$, respectively.

The quality of the state estimation process after the k th data collection is typically based on the error covariance matrix $P_{k|k}$. Combining equations (16) and (17), and by applying the matrix inversion lemma, this matrix can be expressed as

$$P_{k|k} = [P_{k|k-1}^{-1} + C_k^T R_k^{-1} C_k]^{-1}. \quad (18)$$

The main issue of using some function of the covariance matrix as a cost function is that, because of the inversion, this is a nonlinear function of the decision variables γ_k^i .

An alternative to the covariance matrix is the Fisher Information matrix Y_k . This matrix describes the quantity of information associated to each variable, and for the case of a linear system, is equivalent to $Y_{k|k} = P_{k|k}^{-1}$ [26]. Accordingly, the post-information matrix of the estimator can be expressed as

$$Y_{k|k} = P_{k|k-1}^{-1} + C_k^T R_k^{-1} C_k, \quad (19)$$

which provides a simpler expression. Since in this paper the matrix $R_k \in \mathbb{R}^{M_k \times M_k}$ is assumed diagonal matrix, the Fisher information matrix (19) can be simplified as

$$Y_{k|k} = P_{k|k-1}^{-1} + \sum_i^{M_k} \frac{C_{k,i}^T C_{k,i}}{r_{k,i}}, \quad (20)$$

where $r_{k,i}$ is the i -th diagonal entry of the matrix R_k , and $C_{k,i}$ is the observation matrix when only the measurement of the i th entry is available. We can further simplify the expression by separating the contribution from mobile and fixed sensors as

$$Y_{k|k} = P_{k|k-1}^{-1} + \sum_{i=1}^N C_{f,i}^T R_i^f C_{f,i} + \sum_{i=1}^N \gamma_{i,k} (C_{m,i}^T R_i^m C_{m,i}) \quad (21)$$

where $C_{f,i}$ represents the observation matrix C whose only non-zeros entries belong to the fixed measurements of the area i and, similarly, $C_{m,j}$ denotes the matrix C with entries associated to the mobile sensor measurements. In this reformulation the information matrix is conveniently defined as a linear function of the binary variable γ_k^i .

When working with covariance matrices, a common measure of performance is the trace of the covariance matrix. However, in the case of the Fisher information matrix it has been shown [27] that its trace does not distinguish the gains based on the value of the eigenvalues. Therefore the trace fails to provide an appropriate measurement of the information.

In this paper, we propose as a performance objective the maximization of the minimum eigenvalue of the Fisher information matrix which can be synthetically described as

$$\begin{aligned} & \max_{\alpha, \gamma_k^i} \quad \alpha \\ \text{subject to} \quad & P_{k|k-1}^{-1} + \sum_{i=1}^N C_{f,i}^T R_i^f C_{f,i} + \sum_{i=1}^N \gamma_{i,k} (C_{m,i}^T R_i^m C_{m,i}) \geq \alpha I. \end{aligned} \quad (22)$$

In this setting, the problem becomes the one of determining at each time a sequence of nodes S_k satisfying (8)-(12) such that maximizes (22), where $\gamma_{i,k} = 1$ if and only if $i \in S_k$.

It is very important to remark that, thanks to the statistical properties of the Linear Kalman Filter, the covariance, the information matrix and any metric associated to it, do not depend on the actual values of the measurements, but only on the covariance at time $k-1$ and of the sensing structure used at time k .

IV. INFORMATION-BASED ORIENTEERING PROBLEM

The problem described in the previous two sections can be seen as a special Orienteering Problem where we have to select a subset of nodes to be visited and their order so that the information is maximized and the autonomy constraints are satisfied.

In this section, following an approach inspired by the Miller-Tucker-Zemlin (MTZ) formulation of the TSP [28], we will propose a convenient mathematical formulation of this particular Orienteering Problem. To this end, let us introduce two sets of decision variables; i) the binary variable q_{ij} whose value is 1 if the node j is visited after the node i and 0 otherwise, and ii) the integer variable u_i which denotes the visiting order of the node i .

The choice of an initial and final point is enforced by the following constraints

$$\sum_{i=1}^N q_{0i} = \sum_{j=1}^N q_{jN+1} = 1, \quad (23)$$

$$\sum_{i=1}^N q_{i0} = \sum_{j=1}^N q_{N+1j} = 0. \quad (24)$$

For the rest of nodes, we must ensure that each node is visited at most once and that the path obtained is continuous

$$\sum_{i \in N_p} q_{ip} = \sum_{j \in N_p} q_{pj} \leq 1; \quad \forall p = 1, \dots, N, \quad (25)$$

where $N_p = \{i | (i, p) \in E\}$, denotes the set of neighbors of the node $p \in V$. The endurance constraints is formalized as

$$\sum_{i=1}^{N-1} \sum_{j \in N_i} t_{ij} q_{ij} \leq T_{max,k}. \quad (26)$$

To avoid possible subtours and to ensure the continuity of the path, it must hold that

$$2 \leq u_i \leq N \quad \forall i = 1, \dots, N, \quad (27)$$

$$u_i - u_j + 1 \leq (N-1)(1 - q_{ij}) \quad \forall i, j = 2, \dots, N, \quad (i, j) \in E. \quad (28)$$

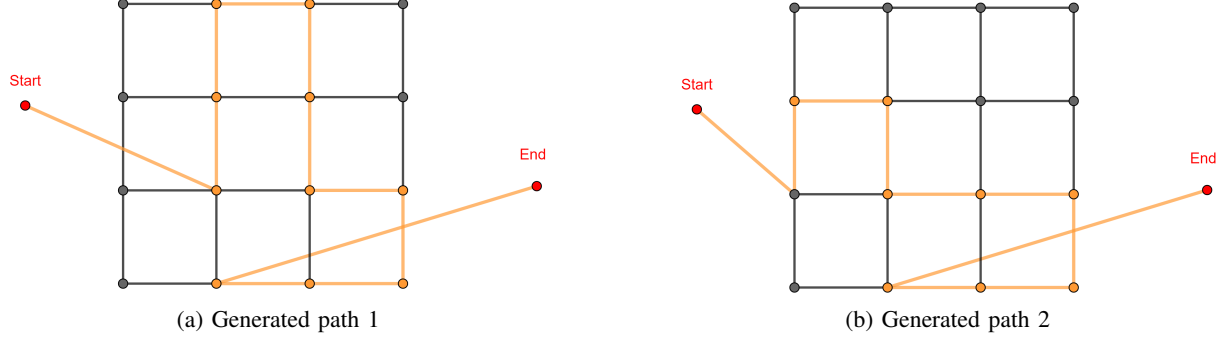


Fig. 3: Examples of feasible paths.

Constraints (23)-(28) ensure the feasibility of the mobile sensor path. Fig. 3 shows two examples of feasible and continuous paths.

Note that the fact of sensing the i th area at time k , previously introduced as $\gamma_{i,k} = 1$, is equivalent to the condition $\sum_{j \in N_i} q_{ji} = 1$. Therefore, combining the path planning integer constraints (23)-(28) with (22), where we substitute $\gamma_{i,k} = \sum_{j \in N_i} q_{ji}$, the following optimization problem is obtained

$$\begin{aligned}
 & \max_{\alpha, q, u} \alpha, \\
 \text{s.t.} \quad & P_{k|k-1}^{-1} + \sum_{i=1}^N C_{f,i}^T R_i^f C_{f,i} + \sum_{i=1}^N \sum_{j \in N_i} q_{ji} (C_{m,i}^T R_i^m C_{m,i}) \geq \alpha I, \\
 & \sum_{i=2}^N q_{1i} = \sum_{j=1}^{N-1} q_{j1} = 1, \\
 & \sum_{i=1}^{N-1} q_{i1} = \sum_{j=2}^N q_{1j} = 0, \\
 & \sum_{i \in N_p} q_{ip} = \sum_{j \in N_p} q_{pj} \leq 1; \quad \forall p = 2, \dots, N-1, \\
 & \sum_{i=1}^{N-1} \sum_{j \in N_i} t_{ij} q_{ij} \leq T_{max,k}, \\
 & 2 \leq u_i \leq N \quad \forall i = 2, \dots, N, \\
 & u_i - u_j + 1 \leq (N-1)(1 - q_{ij}) \quad \forall i, j = 2, \dots, N, \quad (i, j) \in E \\
 & q_{ij} \in \{0, 1\} \quad \forall i, j = 1, \dots, N, \quad (i, j) \in E.
 \end{aligned} \tag{29}$$

In this formulation, the information-based path planning is expressed as a Mixed-Integer Semidefinite Programming (MISDP) problem which, for reasonably small instances of the problem, can be solved optimally using commercial solvers such as *SCIP* or *cutsdp* [29], [30]. Nevertheless, it remains a NP-hard problem whose solving time grows excessively in the case of large instances of the problem.

V. PROPOSED HEURISTIC

In this section we propose two heuristics to compute a suboptimal path based on the integer relaxation of the mixed-integer problem (29). The goal is to obtain close-to-optimal strategies more adequate for large-scale scenarios. Consider $q_{ij} \in [0, 1]$ and $u_i \in \mathbb{R}$ subject to

$$2 \leq u_i \leq N; \quad \forall i = 2, \dots, N. \tag{30}$$

Problem (29) becomes a Semi-Definite Programming (SDP) problem, which can be effectively and quickly solved by solvers such as *Mosek* [31].

The outcome of this convex problem, q_{ij}^r , provides values between 0 and 1 for the edges, see Fig. 4, which can be seen as how likely is the edge (i, j) to be taken in the optimal path. Therefore, a suboptimal solution can be obtained by computing heuristics which select the points to visit based on these values [32].

Algorithm 1 selects the path by rounding up each link (i, j) with probability q_{ij}^r . This greedy approach inserts the new edges into the path based on their probability to be part of the optimal solution. To ensure that the obtained path is feasible and continuous, the rounding is done sequentially. The algorithm starts from the initial point V_{ini} adding edges until the maximum flight time T_{max} is reached. This process is depicted in Fig. 5.

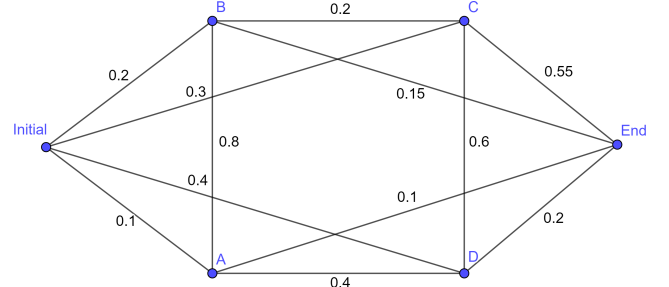


Fig. 4: Example of a possible solution of the relaxed problem.

To converge to a close-to-optimal solution, the operation is repeated for a fixed number of L iterations. After each iteration, the minimum eigenvalue associated to the computed path, $\lambda_1(X_{path})$, is compared with the previously stored solution. If the new path improves the current stored sequence, the latter is replaced and the algorithm keeps seeking for alternative paths.

Algorithm 2 uses a similar approach focusing, instead, on the probability of selecting nodes. For this purpose, the values obtained from the SDP problem are moved towards the nodes as an equivalent of a *reward* value. After the solutions q_{ij}^r are obtained, the reward θ_i for $i \in V$ is computed as

$$\theta_i = \sum_{j \in N_i} q_{ji}^r \quad \forall i \in V \tag{31}$$

Algorithm 1 Sequentially edge randomized rounding

Input: Solution G_{rel}
Output: Set of edges X_{path} where $\lambda_1(X_{path})$ is maximized

- 1: $X_{path} \leftarrow \emptyset$
- 2: **for** $it \leq L$ **do**
- 3: $X_{temp} \leftarrow \emptyset$
- 4: $i \leftarrow ini$ % Start from initial node ini
- 5: **repeat**
- 6: Select q_{ij} by rounding adjacent edges
- 7: $X_{temp} \leftarrow q_{ij}$
- 8: $i \leftarrow j$ % Move to next node i
- 9: **until** ($T_{temp} \geq T_{max}$)
- 10: **return** X_{temp}
- 11: **if** $\lambda_1(X_{temp}) \geq \lambda_1(X_{path})$ **then**
- 12: $X_{path} \leftarrow X_{temp}$
- 13: **end if**
- 14: **end for**
- 15: **Output** X_{path}

where N_i represents the set of nodes that have an edge towards the node i . By performing this operation, we obtain a reward for the visit of each node based on the relaxed problem. The main idea behind this second heuristic is to prioritize the nodes with multiple high valued edges.

The insertion of nodes in the final path is done by following a randomized rounding similar to the one used in Algorithm 1. Therefore, once a node is selected, the next iteration chooses within the neighbouring nodes N_i . The process is repeated for L iterations, comparing the stored values once T_{max} is reached, and starting the process again from the initial node.

Algorithm 2 Sequentially node randomized rounding

Input: Reward $\theta \in \mathbb{R}^N$ and graph G^*
Output: Set of edges X_{path} where $\lambda_1(X_{path})$ is maximized

- 1: $X_{path} \leftarrow \emptyset$
- 2: **for** $it \leq L$ **do**
- 3: $X_{temp} \leftarrow \emptyset$
- 4: $i \leftarrow ini$ % Start from initial node ini
- 5: **repeat**
- 6: Select $V_j \in N_i$ based on θ_j
- 7: $X_{temp} \leftarrow q_{ij}$
- 8: $i \leftarrow j$ % Move to next node i
- 9: **until** ($T_{temp} \geq T_{max}$)
- 10: **return** X_{temp}
- 11: **if** $\lambda_1(X_{temp}) \geq \lambda_1(X_{path})$ **then**
- 12: $X_{path} \leftarrow X_{temp}$
- 13: **end if**
- 14: **end for**
- 15: **Output** X_{path}

VI. COMPUTATIONAL ANALYSIS OF THE HEURISTICS

This section presents a study of the scalability, accuracy, and computational performance of the two presented heuristics respect to the optimal formulation (29).

Simulations are performed given different size areas, ranging from grids of 4×4 up to 6×6 nodes. In order to obtain meaningful results, for each problem size, 100 simulations have been performed varying the information distribution of the process. For this test, the autonomy of the vehicle is such that it allows to visit a maximum of 6 to 9 nodes depending on the size of the grid. This constraint allows to obtain representative differences between the solutions.

Table I provides the level of degradation from both heuristics respect to the optimal value. It is noticeable that both heuristics are able to obtain results with less than 5% of degradation respect to the optimal, while providing outperforming results in terms of computational time, as it is shown in Table II.

TABLE I: Solution degradation between the two proposed strategies and the optimal.

| Grid size | Algorithm 1 | Algorithm 2 |
|--------------|-------------|-------------|
| 4×4 | 4.80% | 4.74% |
| 5×5 | 3.82% | 3.95% |
| 5×6 | 3.46% | 3.75% |

Table II depicts the average time used to obtain the solution to the path-planning problem. In this case, for more than 36 nodes (a grid of 6×6), we can observe how the computational time for the mixed-integer formulation of the problem already increases in an excessive manner. However, for both heuristic strategies, as Fig. 6 shows, they provide reasonable computational times even for larger cases with more than 150 nodes.

TABLE II: Comparison computational time between the optimal and the two proposed strategies.

| Grid size | Algorithm 1 (s) | Algorithm 2 (s) | Optimal (s) |
|--------------|-----------------|-----------------|-------------|
| 4×4 | 1.96 | 1.83 | 8.12 |
| 5×5 | 1.91 | 1.77 | 169.06 |
| 5×6 | 2.20 | 1.72 | 372.58 |
| 6×6 | 2.24 | 2.19 | > 3600 |

These results show that both heuristics, while providing sub-optimal results, achieve a level of performance interestingly close to the optimal. Furthermore, their low computational times are promising in their use in large-scale scenarios.

VII. SIMULATION RESULTS AND APPLICATION

This section provides, through numerical simulations, an illustration of the effectiveness of the information-based path planning introduced in this paper. To do so, the adaptability of the path, the evolution over time and the performance are analysed and compared against a traditional covering strategy.

To provide a more constructive visualisation, the simulations are based on a realistic precision agriculture scenario.

A. Case study: Precision agriculture

The effectiveness of the proposed planning method is shown through a numerical example. In this example we consider an hazelnut orchard where we want to estimate the water content of the plants and soil using the information collected by a

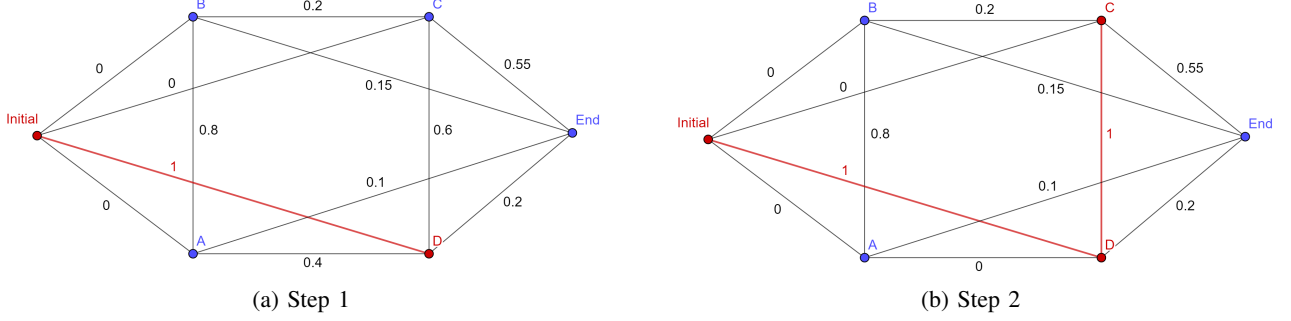


Fig. 5: One step of the randomized rounding algorithm.

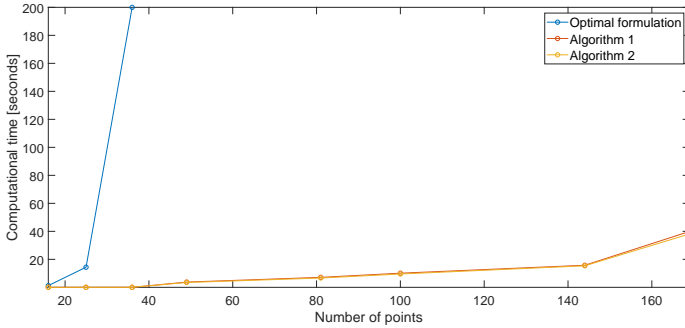


Fig. 6: Evolution of the computational time for the different methods.

drone, a network of fixed soil humidity sensors distributed in the orchard, and of an agrometeorological IoT network providing some climate and rainfall measurements in real time.

In particular we consider an orchard of n plants and N soil parcels, the following system is considered:

$$\begin{cases} x_{k+1} &= Ax_k + Bu_k + B_d\hat{d}_k + w_k \\ y_k &= \Gamma_k(Cx_k + v_k) \end{cases} \quad (32)$$

where $x = [x_1^T \ x_2^T \ x_3^T]^T \in \mathbb{R}^{N+2n}$ is the state vector with $x_1 = [\theta_1, \dots, \theta_N]^T$ the soil moisture status, $x_2 = [W_1, \dots, W_n]^T$ the water plant status and $x_3 = [W_{rem,1}, \dots, W_{rem,n}]^T$ the water status of the leaves, u_k represents the irrigation inputs and \hat{d}_k the meteorological disturbances. The used system dynamics mimic the experimental setting proposed in the PANTHEON project, which comprises a portion of an orchard within the “Azienda Agricola Vignola”, a farm located in the province of Viterbo, Italy. The model and the parameters used to describe the water dynamics are the ones presented in [33]. In this model it is assumed that the fixed sensors are able to capture the value of soil moisture in the area where they are deployed and that the drone is able to measure the water status of the leaves. For further information about the model, the reader is referred to [33].

B. Simulations

In this section, the performance of the path planning is demonstrated. Simulations are carried out for two different distributions of the ground sensors. The two scenarios are

depicted in Fig. 7. Note that the areas close to the fixed sensors have more information about the water states than the more isolated areas. Therefore one can expect that changing the location of the sensors changes the information distribution [16] and thus the optimal covering path.

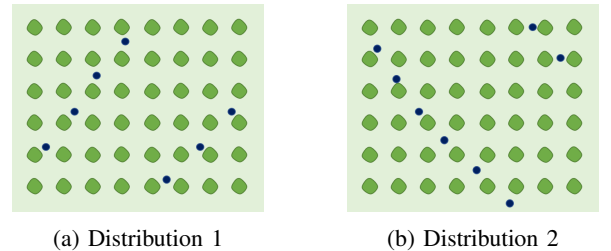


Fig. 7: Fixed sensor distributions.

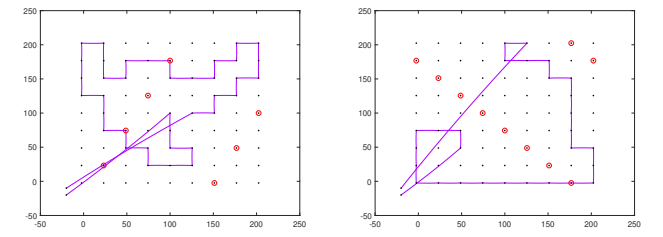


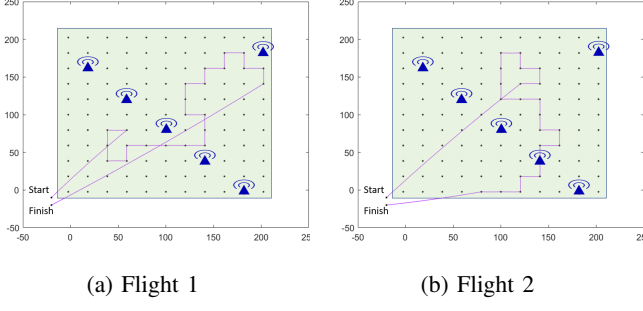
Fig. 8: Comparison of the obtained path according to the soil sensor distribution.

The paths obtained for both distributions are depicted in Fig. 8. These results show how the optimal path changes according to the fixed sensor position.

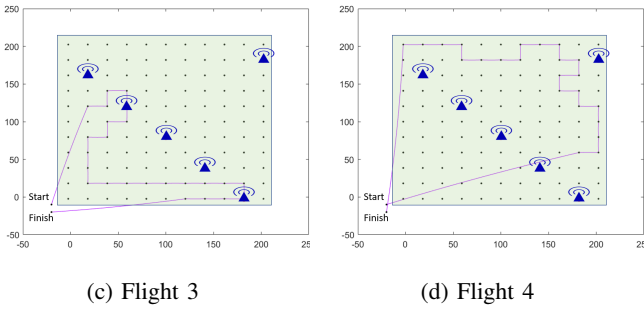
Clearly, the path strongly depends on the information matrix available before the measurement. To highlight this, a small area of an orchard has been simulated and four sampling period considered. The resulting paths are depicted in Fig. 9. As it can be seen from the four plots, the areas with less information change accordingly to the already covered points and so does the path, demonstrating the spatial and temporal awareness of the presented strategy.

C. Performance analysis

In this subsection, an iterative implementation of the presented path planning strategy is compared against a common



(a) Flight 1 (b) Flight 2



(c) Flight 3 (d) Flight 4

Fig. 9: Iterative path evolution.

strategy in persistent monitoring. This strategy divides the area into equal number of partitions based on the flight autonomy. The areas are covered, sequentially ensuring the minimum latency in between visits.

To obtain a fair comparison, the maximum flight time is common for all the sensing strategies.

The model is simulated over an horizon of 350 hours and the data used for the meteorological disturbances comes from direct measurements for the area of Viterbo. The flights are performed with a nonuniform sampling period ranging between 35 and 70 hours, to realistically simulate logistics and weather uncertainty.

First, to include the performance of the optimal strategy proposed in Section IV, a simulation for a simpler grid of 6×6 nodes is performed. In Fig. 10, the evolution of the minimum eigenvalue of the information matrix is shown. In this figure, the traditional strategy is referred as *Arbitrary division* and the heuristic shown corresponds to the Algorithm 1. From this plot, it can be seen that the presented strategies, optimal and suboptimal, clearly provide better results than the regular division.

It is also important to notice how the optimal formulation sometimes is worse than the heuristic strategy (Algorithm 1). This is due to the myopic approach followed in the development of the formulation, which can lead to less favorable situations in the case of short or regular periodicity in the remote sensing.

In Fig. 11 the evolution of the trace of the covariance matrix is depicted. It can be seen that the presented strategies also provide much better results at steady state than the usual arbitrary strategy.

Fig. 13 depicts the results obtained from a larger scenario, where the area dimensions correspond to a real large-scale

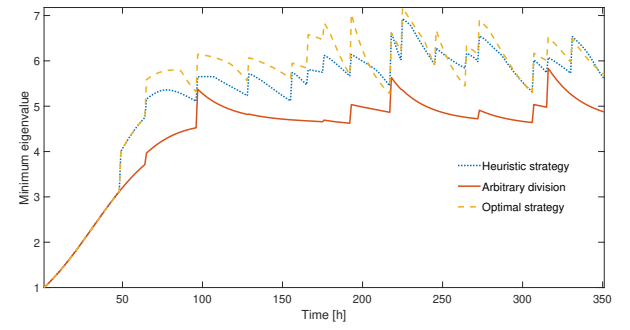


Fig. 10: Evolution of the minimum eigenvalue of the information matrix in a grid of 6×6 nodes.

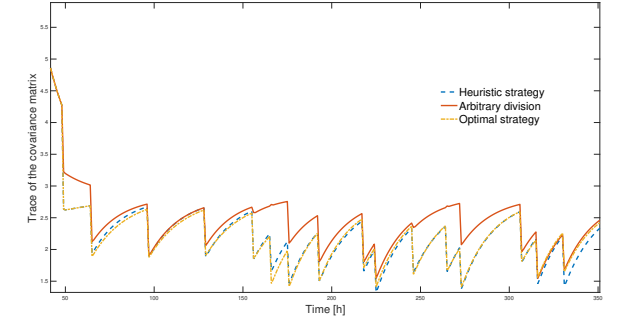


Fig. 11: Evolution of the trace of the covariance matrix in a grid of 6×6 nodes.

hazelnut orchards, as shown in Fig. 12. In this case, the values represented in the plot denote the ratio between the performance of the proposed strategies and the regular division of the area which is computed as

$$R(t) = \frac{\lambda_{1,heur}(t)}{\lambda_{1,arb}(t)}, \quad (33)$$

where $\lambda_1(t)$ represents the minimum eigenvalue at time k of the Fisher information matrix associated to each strategy.



Fig. 12: Area considered for the simulation.

From Fig. 13, we can observe how the heuristic strategies provide at all instants a better performance than the strategy based only on latency between visits. Also, it shows the similar behaviour of both algorithms presented in this paper.

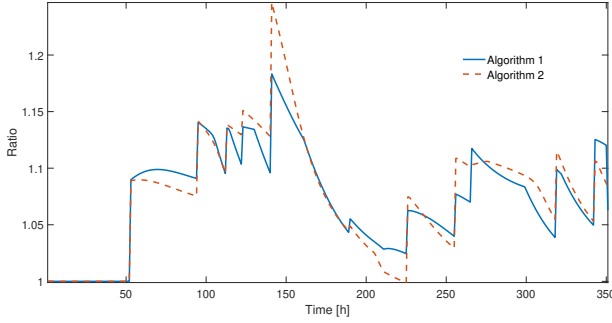


Fig. 13: Ratio between the performance obtained for the different strategies.

Finally, fig. 14 provides, for a similar setup, the case where the maximum flying time for the information-based strategy is reduced by 50%. From this plot, it can be seen that after reducing by 50% the resources, the information-based strategy is still able to outperform most of the time the regular coverage strategy. This result supports one of the main claims of this paper, which is that an information-based approach can help to reduce the resources put into the monitoring while keeping similar performance.

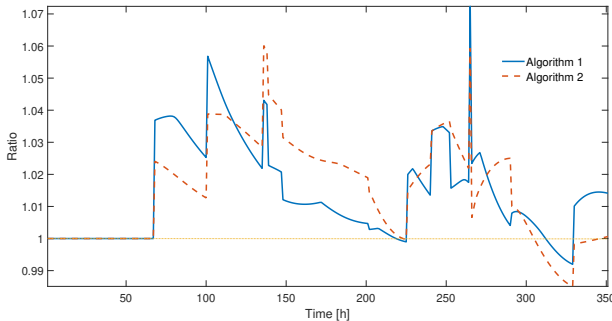


Fig. 14: Evolution of the ratio of performance. Case with reduction of 50% in flying time for the information-based approach.

Remark 1: The results shown in this subsection are obtained in the case of a static sensor distribution and with a fairly symmetric structure. In the case of less symmetric structures the difference between the two approaches becomes larger and even more significant.

VIII. CONCLUSION

This paper presents a novel path planning strategy based on the use of information from a Kalman filter. Focusing on the coverage of large-scale areas, we propose a path computation strategy where the flying time constraint is taken into account and the estimation of the states of the system is maximized. The problem is formulated as a Mixed-Integer Semi-Definite Programming problem which provides an optimal solution. Additionally, we present two primary heuristics with close-to-optimal results.

The effectiveness of the presented strategy is shown through numerical simulations. These simulations demonstrate a clear

improvement in the performance with respect to classical strategies. Moreover, the adaptability and flexibility of this approach not only makes it suitable for fixed sensing structures but also it is a promising step for the combination with a fleet of mobile robots.

Future works will focus on adapting the presented approach to the case where several vehicles as well as an extension to a non-myopic policy for multiple missions with fixed periodicity.

REFERENCES

- [1] L. Santesteban, S. Di Gennaro, A. Herrero-Langreo, C. Miranda, J. Royo, and A. Mateo, "High-resolution UAV-based thermal imaging to estimate the instantaneous and seasonal variability of plant water status within a vineyard," *Agricultural Water Management*, vol. 183, pp. 49–59, Mar. 2017.
- [2] K. Themistocleous, A. Agapiou, B. Cuca, and D. G. Hadjimitsis, "Unmanned Aerial Systems and Spectroscopy for Remote Sensing Applications in Archaeology," *ISPRS - International Archives of the Photogrammetry, Remote Sensing and Spatial Information Sciences*, vol. XL-7/W3, pp. 1419–1423, Apr. 2015.
- [3] Y. Ham, K. K. Han, J. J. Lin, and M. Golparvar-Fard, "Visual monitoring of civil infrastructure systems via camera-equipped Unmanned Aerial Vehicles (UAVs): a review of related works," *Visualization in Engineering*, vol. 4, Dec. 2016.
- [4] I. Colomina and P. Molina, "Unmanned aerial systems for photogrammetry and remote sensing: A review," *ISPRS Journal of Photogrammetry and Remote Sensing*, vol. 92, pp. 79–97, June 2014.
- [5] M. Daz-Cabrera, J. Cabrera-Gmez, R. Aguasca-Colomo, and K. Miatliuk, "Photogrammetric Analysis of Images Acquired by an UAV," in *Computer Aided Systems Theory - EUROCAST 2013* (R. Moreno-Daz, F. Pichler, and A. Quesada-Arenzibia, eds.), (Berlin, Heidelberg), pp. 109–116, Springer Berlin Heidelberg, 2013.
- [6] S. Alamdari, E. Fata, and S. L. Smith, "Persistent Monitoring in Discrete Environments: Minimizing the Maximum Weighted Latency Between Observations," *arXiv:1202.5619 [cs]*, Feb. 2012. arXiv: 1202.5619.
- [7] C. G. Cassandras, X. Lin, and X. Ding, "An Optimal Control Approach to the Multi-Agent Persistent Monitoring Problem," *IEEE Transactions on Automatic Control*, vol. 58, pp. 947–961, Apr. 2013.
- [8] J. Scherer and B. Rinner, "Persistent Multi-UAV Surveillance with Data Latency Constraints," *arXiv:1907.01205 [cs, eess]*, July 2019. arXiv: 1907.01205.
- [9] A. T. Klesh, P. T. Kabamba, and A. R. Girard, "Path planning for cooperative time-optimal information collection," in *2008 American Control Conference*, (Seattle, WA), pp. 1991–1996, IEEE, June 2008.
- [10] K.-C. Ma, Z. Ma, L. Liu, and G. S. Sukhatme, "Multi-robot Informative and Adaptive Planning for Persistent Environmental Monitoring," in *Distributed Autonomous Robotic Systems* (R. Gro, A. Kolling, S. Berman, E. Frazzoli, A. Martinoli, F. Matsuno, and M. Gauri, eds.), vol. 6, pp. 285–298, Cham: Springer International Publishing, 2018.
- [11] R. Cui, Y. Li, and W. Yan, "Mutual Information-Based Multi-AUV Path Planning for Scalar Field Sampling Using Multidimensional RRT*," *IEEE Transactions on Systems, Man, and Cybernetics: Systems*, vol. 46, pp. 993–1004, July 2016.
- [12] S. Z. Kang and X. T. Hu, "Soil water distribution, uniformity and water-use efficiency under alternate furrow irrigation in arid areas," p. 10.
- [13] T. H. Skaggs, T. J. Trout, and Y. Rothfuss, "Drip Irrigation Water Distribution Patterns: Effects of Emitter Rate, Pulsing, and Antecedent Water Mention of products and trade names are for the benefit of the reader and do not imply a guarantee or endorsement of the product by USDA," *Soil Science Society of America Journal*, vol. 74, no. 6, pp. 1886–1896, 2010. Place: Madison, WI Publisher: Soil Science Society.
- [14] M. Saidan, G. Albaali, e. alasis, and J. Kaldellis, "Experimental study on the effect of dust deposition on solar photovoltaic panels in desert environment," *Renewable Energy*, vol. 92, pp. 499–505, July 2016.
- [15] B. Weber, A. Quiones, R. Almanza, and M. D. Duran, "Performance Reduction of PV Systems by Dust Deposition," *Energy Procedia*, vol. 57, pp. 99–108, 2014.
- [16] V. Tzoumas, A. Jadbabaie, and G. J. Pappas, "Sensor Placement for Optimal Kalman Filtering: Fundamental Limits, Submodularity, and Algorithms," *arXiv:1509.08146 [cs, math]*, Sept. 2015. arXiv: 1509.08146.

- [17] S. Joshi and S. Boyd, "Sensor Selection via Convex Optimization," *IEEE Transactions on Signal Processing*, vol. 57, pp. 451–462, Feb. 2009.
- [18] J. Binney, A. Krause, and G. S. Sukhatme, "Optimizing waypoints for monitoring spatiotemporal phenomena," *The International Journal of Robotics Research*, vol. 32, pp. 873–888, July 2013.
- [19] S. Garg and N. Ayanian, "Persistent Monitoring of Stochastic Spatio-temporal Phenomena with a Small Team of Robots," *arXiv:1804.10544 [cs, stat]*, Apr. 2018. arXiv: 1804.10544.
- [20] X. Lan and M. Schwager, "Planning periodic persistent monitoring trajectories for sensing robots in Gaussian Random Fields," in *2013 IEEE International Conference on Robotics and Automation*, (Karlsruhe, Germany), pp. 2415–2420, IEEE, May 2013.
- [21] B. L. Golden, L. Levy, and R. Vohra, "The orienteering problem," *Naval Research Logistics*, vol. 34, pp. 307–318, June 1987.
- [22] J. Yu, M. Schwager, and D. Rus, "Correlated Orienteering Problem and its Application to Persistent Monitoring Tasks," *IEEE Transactions on Robotics*, vol. 32, pp. 1106–1118, Oct. 2016.
- [23] L. Bottarelli, M. Bicego, J. Blum, and A. Farinelli, "Orienteering-based informative path planning for environmental monitoring," *Engineering Applications of Artificial Intelligence*, vol. 77, pp. 46–58, Jan. 2019.
- [24] B. Sinopoli, L. Schenato, M. Franceschetti, K. Poolla, M. Jordan, and S. Sastry, "Kalman Filtering With Intermittent Observations," *IEEE Transactions on Automatic Control*, vol. 49, pp. 1453–1464, Sept. 2004.
- [25] E. Garone, B. Sinopoli, A. Goldsmith, and A. Casavola, "LQG Control For MIMO Systems Over multiple TCP-like Erasure Channels," p. 15.
- [26] M. Segal and E. Weinstein, "A new method for evaluating the log-likelihood gradient, the Hessian, and the Fisher information matrix for linear dynamic systems," *IEEE Transactions on Information Theory*, vol. 35, pp. 682–687, May 1989.
- [27] B. Grocholsky, "Information-Theoretic Control of Multiple Sensor Platforms," p. 199.
- [28] C. E. Miller, A. W. Tucker, and R. A. Zemlin, "Integer Programming Formulation of Traveling Salesman Problems," *Journal of the ACM*, vol. 7, pp. 326–329, Oct. 1960.
- [29] T. Gally, M. E. Pfetsch, and S. Ulbrich, "A framework for solving mixed-integer semidefinite programs," *Optimization Methods and Software*, vol. 33, pp. 594–632, May 2018. Publisher: Taylor & Francis.
- [30] C. Rowe and J. Maciejowski, "An efficient algorithm for mixed integer semidefinite optimisation," in *Proceedings of the 2003 American Control Conference, 2003.*, vol. 6, pp. 4730–4735 vol.6, June 2003. Journal Abbreviation: Proceedings of the 2003 American Control Conference, 2003.
- [31] L. Vandenberghe and S. Boyd, "Semidefinite Programming," *SIAM Review*, vol. 38, pp. 49–95, Mar. 1996. Publisher: Society for Industrial and Applied Mathematics.
- [32] P. Raghavan and C. D. Tompson, "Randomized rounding: A technique for provably good algorithms and algorithmic proofs," *Combinatorica*, vol. 7, pp. 365–374, Dec. 1987.
- [33] N. Bono Rossello, R. Fabrizio Carpio, A. Gasparri, and E. Garone, "A novel Observer-based Architecture for Water Management in Large-Scale (Hazelnut) Orchards," *IFAC-PapersOnLine*, vol. 52, no. 30, pp. 62–69, 2019.